Optics Communications 283 (2010) 474–479

Contents lists available at ScienceDirect

Optics Communications

journal homepage: www.elsevier.com/locate/optcom

All optical Flip-Flop based on a nonlinear DFB semiconductor laser: Theoretical study

Hossam Zoweil *, A.B. Kashyout

Advanced Technology and New Materials Research Institute, Mubarak City for Scientific Research and Technology Applications, P.O. Box 21934, New Borg El-Arab City, Alexandria, Egypt

ARTICLE INFO

Article history:
Received 13 September 2009
Received in revised form 14 October 2009
Accepted 15 October 2009

PACS:
42.65.Pc
42.55.Px

Keywords:
All optical switching
Flip-Flop
DFB semiconductor laser
Nonlinear refractive index

ABSTRACT

A new design of an all optical Flip-Flop is proposed. It consists of a nonlinear distributed feedback (DFB) laser. The wave guiding layer of the DFB laser consists of linear grating section followed by a nonlinear one, and both sections are separated by a phase shift section. In the OFF-state, the real part of the refractive index in the wave guiding layer forms a Bragg grating. In the ON-state, it forms a Bragg grating with a phase shift section. Optical gain is achieved by current injection in the semiconductor active layer. Nonlinearity in the nonlinear layers of the semiconductor grating was achieved by direct absorption at the edge of the absorption band (Urbach tail). Numerical simulation shows that the device switches in a nanosecond time scale.

1. Introduction

Optical internet has generated large interests in all optical switching devices and systems. Processing data in the optical domain eliminates the need to optical to electronics and electronics to optical data conversion, which means faster and cheaper optical internet routing. All optical packet switching is a preferred way for all optical routing and processing of data. It requires the use of all optical Flip-Flop elements. Many devices/systems were investigated to achieve all optical Flip-Flop operation [1–6]. For example in [4], two semiconductor optical amplifiers (SOA), two ring cavities, and two optical filters are required to build a Flip-Flop. In [5] a vertical cavity semiconductor optical amplifier (VCSOA) and a holding beam are required to achieve all optical Flip-Flop. In [6] a single DFB laser and a holding beam are required for an all optical Flip-Flop operation, and the operation depends on charge dynamics in the active layer. In this paper, an all optical Flip-Flop based on a single periodic nonlinear grating semiconductor laser is proposed. It does not require a holding beam which means less hardware, and less complexities. The guiding layer of the suggested device consists of a compound nonlinear grating with periodic nonlinearity. The switching dynamics depend on (a) charge dynamics in the guiding layer to induce a grating, and (b) charges dynamics in the active layer to switch the device off. Nonlinear periodic structures with periodic nonlinearity were studied intensively [7–13]. A photonics bandgap material of alternative layers of linear and nonlinear dielectrics was investigated in [7]. It showed all optical limiting and all optical switching. A grating structure containing periodic layers of positive then negative Kerr nonlinearity was studied by Brzozowski et al. [8], Fig. 1a. Also, a nonlinear grating with a periodic nonlinearity was investigated in [14], Fig. 1b. In this structure, the layer of a high refractive index exhibits a negative Kerr nonlinearity and the layer of a low refractive index exhibits a positive Kerr nonlinearity. This structure was built using semiconductor materials [15], where quantum well structure was used in each layer to achieve negative and positive nonlinear coefficients. All these structures switch an optical signal at the edge of the grating bandgap. A structure that switches an optical signal within the bandgap of the grating is introduced in [16]. The structure consists of a linear grating section *A* followed by a nonlinear grating section *B* as shown in Fig. 2. When low light intensity is injected into the structure, the nonlinearity of the grating has no effect, when a high light intensity signal is injected into the grating, the grating structure in the nonlinear section is flipped over, and the nonlinear section is shifted by $\pi/2$ from the linear section. This phase shift opens a narrow transmission band within the reflection band of the grating. For a DFB laser, the gain

* Corresponding author. Tel./fax: +203 4593414.
E-mail address: zoweil@gmail.com (H. Zoweil).

0030-4018/$ - see front matter © 2009 Elsevier B.V. All rights reserved.
doi:10.1016/j.optcom.2009.10.031

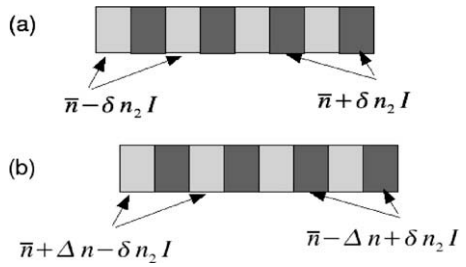

Fig. 1. (a) Structure described in [8] and (b) structure in [14].

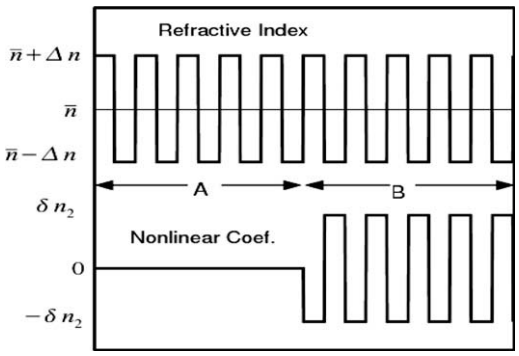

Fig. 2. Nonlinear grating structure in [16].

threshold of a phase shifted grating is less than that of a grating without a phase shift. It is possible to add optical gain to the structure in Fig. 2 such that at low light intensity in the structure, when the nonlinearity does not change the grating coupling in the nonlinear section, the gain is below threshold and the device is in the nonlasing state (OFF-state). When high light intensity exists in the structure, the nonlinearity in the nonlinear section reverses the periodic variation in refractive index, and a phase shift exists in the structure. In this case, the gain is above threshold, and the device is in the lasing state (ON-state). The structure shown in Fig. 2 requires layers of negative and positive nonlinear Kerr coefficients with same absolute value at the same wavelength, which is difficult to achieve. In this paper, another structure is proposed in Fig. 3. The nonlinear section of the grating is implemented by successive of linear and nonlinear layers with negative nonlinearity. The need of both types of nonlinearity (positive and negative nonlinearities as in [15]) is eliminated. The nonlinearity proposed is due to direct absorption at the edge of the absorption band (Urbach tail), which is easier to achieve than the nonlinearity due to quantum well structures. The optical gain is achieved by

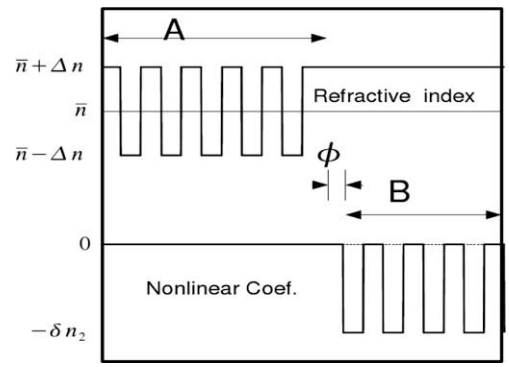

Fig. 3. Suggested structure.

current injection into an active semiconductor layer. The switching from one state (OFF-state/ON-state) to the second state (ON-state/OFF-state) is done by all optical means. In the following sections, the structure of the device is described. Materials required are discussed. A set of equations describing fields propagation coupled with gain and carrier generation in nonlinear grating layers is introduced. All optical set–reset operation is shown in a numerical simulation.

2. Theory and analysis

2.1. Device description

The suggested nonlinear structure that comprises only negative nonlinearity is shown in Fig. 3. The first section, *A*, is a linear grating, the second section, *B*, is a periodic distribution of a nonlinear coefficient. This nonlinear coefficient is due to direct absorption at the edge of the absorption band (Urbach tail). The grating period in the second section is equal to the grating period of the first section. The loss grating in the second section is shifted by $\phi = \pi/2$ from the first section. The refractive index in the second section is $\overline{n} + \Delta n$. When a low light intensity is sent through the structure, there is no change in the refractive index of the structure. When high light intensity is sent through the structure, the nonlinear section creates another Bragg grating phase shifted from the first section. An active gain medium is added to the structure to form a semiconductor optical amplifier/laser as shown in Fig. 4. The 3D schematic of the nonlinear DFB laser device is shown in Fig. 5.The optical gain is adjusted so that, at low light intensity inside the structure, the distribution of refractive index and loss does not afford enough feedback to start lasing. The cavity has a low quality factor Q. At high light intensity inside the structure, a refractive index grating is generated in the nonlinear section, and it is phase shifted from the grating in the linear section. The resulted phase shifted grating ensures an enough optical feedback to start lasing. The quality factor of the cavity Q is increased. The high field intensity sent through the cavity switches Q from low to a high value.

To switch the laser mode off, the optical gain in the cavity is reduced by cross gain modulation (XGM). An optical pulse of a

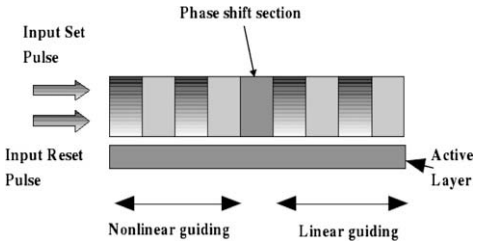

Fig. 4. Suggested Flip-Flop.

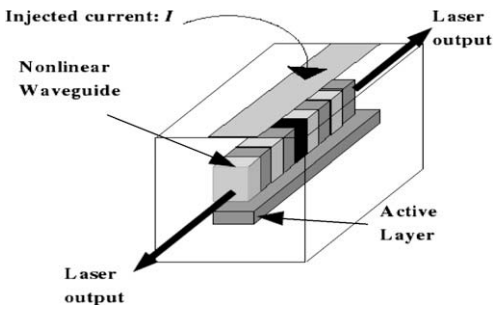

Fig. 5. Schematic of suggested device.

photon energy much lower than the semiconductor bandgap edge reduces the gain of the laser mode and does not generate significant number of electron–hole pairs in the nonlinear layers. The free carriers in the nonlinear layers generated from the decaying laser mode power are reduced in numbers. The refractive index grating coupling in the nonlinear section is reduced. The Q factor of the cavity decreases to its initial low value and the laser mode is switched off.

2.2. Materials consideration

The operation of the device requires a material with high optical negative nonlinearity. This ensures that the optical set/reset signal has a low energy/power. Free carriers injected into the semiconductors leads to a significant change in the loss coefficient above the semiconductor absorption bandgap edge. This change in the loss coefficient leads to a large change in refractive index at the semiconductor absorption band edge [17,18]. This phenomenon was used, for example, to tune a two dimensional silicon photonic band gap (PBG) materials, where the controlling signal was at 1.3 μm, and the photonic band gap edge at 1.5 μm was tuned [19]. The loss coefficient at energies of few tenths of electron volts below to the band edge (Urbach tail) does not change much by the level of free carriers density injected [18]. It was assumed constant in the simulations. The absorption coefficient at a semiconductor band gap edge could be modelled as $\alpha = \alpha_0 exp((\hbar\omega - \hbar\omega_g)/E_0)$ [20]. α_0 is the direct absorption at $\hbar\omega = \hbar\omega_0$. $\hbar\omega$ is the incident photon energy, $\hbar\omega_g$ is the semiconductor band gap energy. E_0 depends on the doping level (N-type, P-type or both). For example, E_0 varies from 0.005 to 0.03 eV for a doping level up to 10^{20} cm^{-3} in *GaAs* [21]. The operating frequency of the device should be just below the absorption band edge of the semiconductor where the free carriers injected by direct absorption lead to a large change in the refractive index. In the simulation, operating frequency at ~ 0.1 eV below the band edge is assumed. For example, at the band gap, i.e. $\hbar\omega = \hbar\omega_g$, consider $\alpha = 40,000\ \text{cm}^{-1}$. To achieve $\alpha = 40\ \text{cm}^{-1}$ at $\hbar\omega - \hbar\omega_g = 0.1$ eV, then E_0 has to be around 0.014 eV. There are two ways to adjust the absorption coefficient at the edge of the absorption band to the desired value: (a) by doping these layers by P-type materials or N-type materials or both of them, this doping changes E_0, (b) by altering E_g. E_g is altered by using a semiconductor alloy (for example;*InGaAsP*) to build the grating. Changing the percentage of the alloy materials changes the value of E_g. In this work, it is assumed that the nonlinear layers have a semiconductor of a bandgap of ≈ 0.9 eV, and the operating frequency is at ≈ 0.1 eV below the band edge, which corresponds to ≈ 1.5 μm. The proposed device could be built from an *InGaAsP* alloy on an *InP* substrate. By varying the alloy materials ratios, the gain spectrum could be adjusted as well as the nonlinearity at the operating frequency in the guiding layer. The nonlinear section of the grating has a constant real refractive index along the propagation direction at low optical field inside. This configuration could be implemented by (a) implementing a nonlinear waveguide with the appropriate cross section adjusted for the required propagation constant at low optical field inside, (b) etching the nonlinear waveguide periodically to get space for the linear layers to be deposited, (c) depositing the linear layers by a deposition technique (for example:metal organic vapor phase epitaxy, MOVPE) and (d) adjusting the cross section area of each linear layer so that its effective propagation constant is equal to the propagation constant in the nonlinear layers at low field inside. A numerical technique (for example, beam propagation method) could be used to predict the required geometry and cross section area of layers in the nonlinear grating to achieve the refractive index distribution required.

2.3. Model

Slow wave approximations were assumed. The electric field in the device has the form:

$E(z,t) = E_+(z,t)e^{-i\beta z + i\omega t} + E_-(z,t)e^{+i\beta z + i\omega t} + c.c.$. Coupled mode equations lead to the following fields equations [22]:

$$i\frac{\partial E_+}{\partial z} + i\frac{\bar{n}}{c}\frac{\partial E_+}{\partial t} = \left(\Gamma_1 + i\frac{g}{2}(1 - i\Gamma) - i\frac{\alpha_{cav}}{2}\right)E_+ - e^{-i\phi(z) - i2\Delta\beta z}(K + \Gamma_2)E_-, \quad (1)$$

$$-i\frac{\partial E_-}{\partial z} + i\frac{\bar{n}}{c}\frac{\partial E_-}{\partial t} = \left(\Gamma_1 + i\frac{g}{2}(1 - i\gamma) - i\frac{\alpha_{cav}}{2}\right)E_- - e^{i\phi(z) + i2\Delta\beta z}(K + \Gamma_2)E_+, \quad (2)$$

$$\Gamma_1 = -\frac{2\pi}{\lambda_G}\left(\Delta n + \left(\frac{\delta n}{\delta N_c}\right)(1 - i\xi)N_c\right) - i\frac{\alpha}{4} \quad \text{for } 0 < z < L/2, \text{ zero otherwise}, \quad (3)$$

$$\Gamma_2 = -\frac{4}{\lambda_G}\left(\frac{\delta n}{\delta N_c}\right)(1 - i\xi)N_c - i\frac{\alpha}{2\pi} \text{for } 0 < z < L/2, \text{ zero otherwise}, \quad (4)$$

$$\frac{\partial N_c}{\partial t} = -\frac{N_c}{\tau_{car}} - BN_c^2 - CN_c^3 + \frac{\alpha I_{int}}{\hbar\omega}, \quad (5)$$

$$\frac{\partial N_g}{\partial t} = \frac{I}{eV} - \frac{N_g}{\tau} - BN_g^2 - CN_g^3 - v_g\Theta gS, \quad (6)$$

$$K = \frac{4\Delta n}{\lambda_G}, \text{ for } L/2 < z < L, \text{ zero otherwise}, \quad (7)$$

$$g = \frac{\tilde{g}(N_g - N_{gtr})}{1 + \epsilon S}, \quad (8)$$

I_{int} is the fields intensities. N_c is the density of carriers in the nonlinear semiconductor layers. N_g is the carrier density in the active layer. α is the direct absorption loss in each semiconductor layer, S is the photon density, and e is the electron charge. $\delta n/\delta N_c = 10^{-26}$ m^3 is the differential change in refractive index due to free electron–hole carriers density injection in the semiconductor at incident photon energy of $\simeq 0.828$ eV (1.5 μ m) [17]. $\xi = 0.033$ is the ratio of induced imaginary part of refractive index to the change in the real part due to free carrier injection [23]. $\Delta n = 0.003$ $\phi = \pi$, for $L/2 < z < L$, zero otherwise. $\lambda_G = 1.5$ μm. Simulation parameters are shown in Table 1.

The coupled equations are solved using Range–Kutta techniques. The device structure is divided into 20 sections. In each section, spontaneous emission fields are added to both the forward and backward fields in the fields equations. No reflection is

Table 1
Simulation parameters.

Symbol	Description	Value
α	Band tail absorption at 1.5 μm	80 cm^{-1}
	Band tail absorption at 1.53 μm	28.8 cm^{-1}
α_{cav}	Cavity loss	25 cm^{-1}
τ_{car}	Recombination time in nonlinear layer	1 ns
τ	Recombination time in active layer	3 ns
ϵ	Gain saturation	1.5×10^{-23} m^3
V	Cavity volume	0.36×10^{-16} m^3
Θ	Overlap factor	0.35
v_g	Group velocity	10^8 m/s
γ	linewidth enhancement	−0.5
B	Radiative recombination	10^{-16} m^3/s
C	Auger recombination	3×10^{-40} m^6/s
I	Injected current	31.08 mA
$\tilde{g}$	Differential gain	4×10^{-20} m^2
N_{gtr}	Transparency carrier density	10^{24} m^{-3}
$\bar{n}$	Average refractive index	3
L	Cavity length	250 μm

assumed from both faces of the device. The input set–reset pulses are sent into the face of the nonlinear section B at $z = 0$.

3. Simulation results

In the simulations, the field power is normalized to $P_0 = 1.352$ mW. Also, N_c is normalized to a carrier density in the guiding layer of $N_{c0} = 6 \times 10^{23}$ m^{-3}. N_g was normalized to $N_{g0} = N_{gtr}$. The coupled mode equations are solved in OFF-state (no input fields) for about 8 ns, the output optical field power from the linear side is shown in Fig. 6.

3.1. Set operation

An optical pulse of 13.52 mW, 250 ps width (3.38 picojoule), and 1.5 μm wavelength switches the device into the ON-state, Fig. 7. The optical pulse generates free electron–hole carriers in the nonlinear grating layers in the guiding layers. These generated carriers reduce refractive index at photon energies close to the absorption band gap edge of the semiconductor. A refractive index Bragg grating is induced in the nonlinear section. This induced grating is phase shifted ($\pi/2$) from the grating in the first section and it provides enough optical feedback for laser mode to build up. The laser mode generates enough electron–hole carriers in the nonlinear layer to maintain the induced grating.

The simulation time was 8 ns. The carrier densities generated in the nonlinear section of the guiding layer at $z = 0$ and at $z = L/2$ are shown in Fig. 8; curves (a), and (b). High carriers densities in the guiding layer at $z = L/2$ is due to laser field concentration around the phase shift section. Free carriers generation in nonlinear layers is required to set the device ON. In the simulation, a pulse at 1.5 μm was used. However, it is possible to use pulse at a photon energy higher than the semiconductor band gap of the nonlinear layer to generate carriers. The carriers densities in the active region are shown in Fig. 8, curves (c), and (d). The transmitted optical power is shown in Fig. 9.

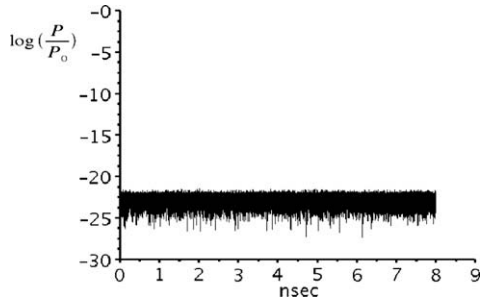

Fig. 6. Output field (linear side), OFF-state.

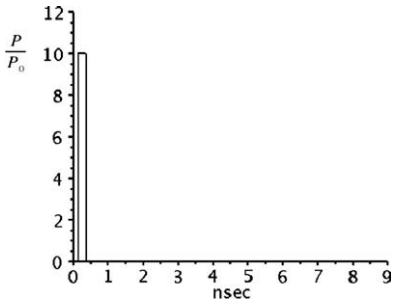

Fig. 7. Input pulse (set operation).

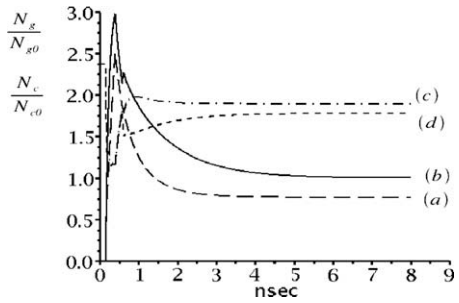

Fig. 8. Carriers densities N_c at (a) $z = 0$, (b) $z = L/2$, N_g, at (c) $z = 0$ and (d) $z = L/2$ (set operation).

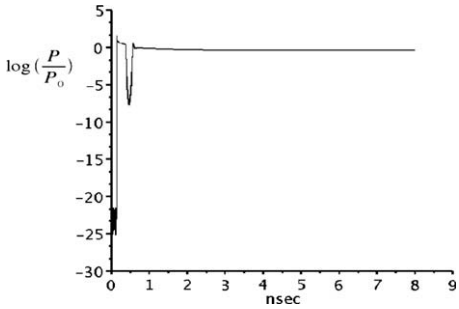

Fig. 9. Output optical power from linear side (set operation).

3.2. Reset operation

Using cross gain modulation (XGM) the output of the laser is switched from ON-state to OFF-state. An optical pulse of 13.52 mW power, and 250 ps width switches the device ON, than an optical pulse of width 3.75 ns, and peak power of 1.352 mW (3.06 picojoule) switches the device OFF, Fig. 10. The last pulse is tuned at photon wavelength of 1.53 μm, which is 0.015 eV less than the set pulse photon energy. Consider that the loss at the band tail in the form of $\alpha = \alpha_0 exp((E - E_g)/E_0)$, if $E_0 = 0.015$ eV, then the loss at reset pulse wavelength (1.53 μm) is 0.36 times the loss at the set pulse wavelength (1.5 μm). In that case, the second optical pulse reduces the optical gain inside the cavity below threshold, and does not generate much free electron–hole pairs in the nonlinear semiconductor layers. It was assumed in the simulations that the optical gain at the reset pulse wavelength (1.53 μm) is half the gain at the set pulse wavelength (1.5 μm). As a consequence, the laser mode decays fast as shown in Fig. 11. The width of the reset pulse is chosen to be greater than τ_{car}, to insure that the carrier density in the nonlinear layer will decay, Fig. 12, and the induced

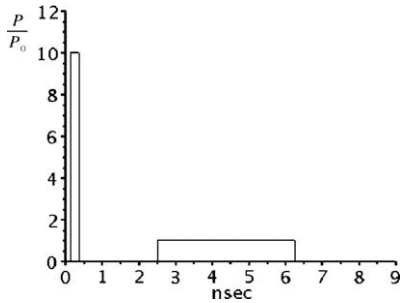

Fig. 10. Input pulses for set–reset simulations.

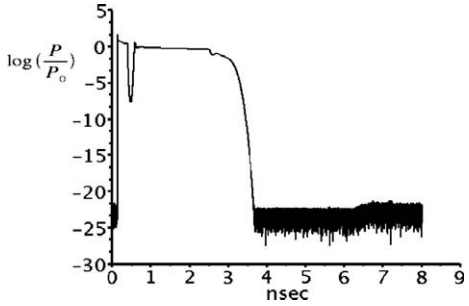

Fig. 11. Optical power output from linear section (set–reset operation).

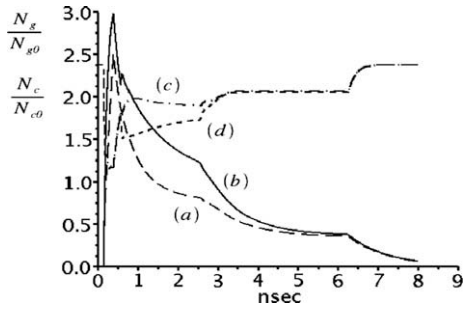

Fig. 12. Carriers densities N_c at (a) $z = 0$, (b) $z = L/2$, N_g at (c) $z = 0$ and (d) $z = L/2$ (set–reset operation).

refractive index grating in the nonlinear section will decrease. In the simulations, it was assumed that the reset pulse generates free electron–hole pair due to a direct absorption loss in the nonlinear guiding layer of 28.8 cm^{-1} at wavelength 1.53 μm.

3.3. Transmission spectrum

Small signal transmission/gain in the 'OFF' and 'ON' state is calculated. First, time domain simulations of the forward and backward propagating fields in the 'OFF' state are performed for 7.5 ns until the carriers densities in the active layer and nonlinear layers become stable. Next, optical gain is calculated according to the carriers densities generated at 7.5 ns in the active layer, and grating coupling in the nonlinear section is calculated according to the carrier density in nonlinear layers at 7.5 ns. Both optical gain and coupling coefficient are used to calculate small signal power gain or transmission for $\delta\beta/K = -8$ to 8. At the output end of the device, it was assumed zero backward field, and only forward field exists. By backward integration using Rang–Kutta technique, the forward and backward fields at the input of the device were calculated. During integration it was assumed that the fields do not

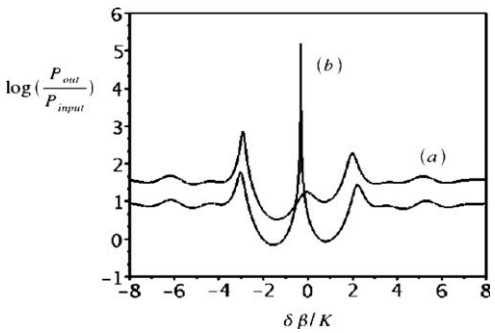

Fig. 13. Small signal power transmission/gain at (a) OFF-state and (b) ON-state.

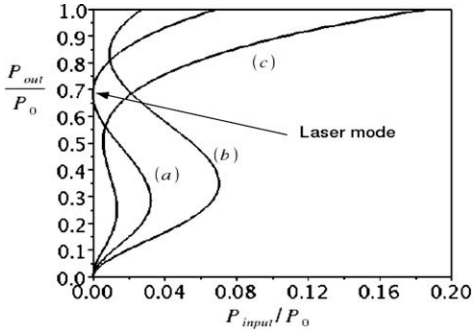

Fig. 14. Bistability at (a) $\delta\beta/K = -0.3$, (b) $\delta\beta/K = -0.2$ and (c) $\delta\beta/K = -0.4$.

change the carriers densities along the device because of its small magnitudes. The transmission is shown in Fig. 13. In the OFF-state the transmission spectrum shows the reflection band of the grating. In the ON state a large peak gain exists at $\delta\beta/K = -0.3$, which corresponds to the laser mode frequency in the ON state. The small signal gain outside the grating reflection band is reduced in the ON state, this is due to the decrease in the carrier density in the active layer when the laser mode is turned ON.

3.4. Steady state optical bistability

The relation between normalised input optical power and normalised output optical power at different values of $\delta\beta/K$ is shown in Fig. 14. The calculations were done in steady state were output normalised optical power is assumed to increase from 0 to 0.2. The backward field at the output is assumed to be zero. From the forward and backward fields the densities of carriers in the active layer and the nonlinear guiding layers were calculated by solving for the root of the cubic algebraic equations of carriers rate equations in steady state. Using Range–Kutta techniques and by backward integration, the input optical power is calculated at the input end of the device. When the input field detuned by $\delta\beta/K = -0.3$, the bistability loop shows the laser mode; the upper branch of the loop touches the output axis ($P_{out}/P_0 \simeq 0.67$) at zero input power. Hence at zero input power, the normalised output laser normalised power is $\simeq 0.67$. The Flip-Flop switches to On state at input normalised optical power of 0.032. When input field was detuned by $\delta\beta/K = -0.2$ and -0.4, the bistability loops do not touch the output axis. The results of steady state calculations of optical output power versus optical input power at $\delta\beta/K = -0.3$ agrees with the spectrum of small signal power gain where the peak optical gain in the ON state occurs at the same detuning frequency $\delta\beta/K = -0.3$.

4. Discussion

The device is switched from ON-state to OFF-state using cross gain modulation. The reset optical pulse reduces the gain in the cavity. In the same time, this pulse produces electron–hole pairs by direct absorption at the edge of Urbach tail. This is due to the fact that the pulse photon energy is just 0.015 eV below the set pulse photon energy. It is important that the electron–holes generation by the reset pulse are reduced, so that it does not induce a grating coupling in the nonlinear section. By using active layer with a wide gain bandwidth, the reset pulse wavelength could be chosen to lie on the lower end of the Urbach tail where the direct absorption is almost negligible. In this case the reset pulse photon energy could be much lower than the set pulse photon energy (for example, 50–60 nm lower), and it can reduce the optical gain by reducing carriers densities in the active layer.

5. Conclusion

A compact all optical Flip-Flop based on a nonlinear semiconductor periodic guiding layer in a semiconductor laser is proposed and simulated in time domain. The device does not require a holding beam to operate. The high nonlinearity due to direct absorption at the band tail insures low optical set/reset pulse energy. Also, it insures low injection current in the active layer. A set pulse at 1.5 μm and a reset pulse at 1.53 μm switch the Flip-Flop ON and OFF in nanosecond time scale. The device could be implemented using *InGaAsP* alloy on an *InP* substrate.

References

[1] H.J.S. Dorren et al., J. Lightw. Technol. 21 (1) (2003) 2.
[2] F. Ramos et al., J. Lightw. Technol. 23 (10) (2005) 2993.
[3] J. Herrera et al., IEEE Photon. Technol. Lett. 19 (13) (2007) 990.
[4] J. Herrera et al., IEEE J. Sel. Top. Quant. Electron. 14 (3) (2008) 808.
[5] A. Kaplan, G. Agrawal, D. Maywar, Electron. Lett. 45 (2) (2009) 808.
[6] K. Huybrechts, G. Morthier, R. Baet, Opt. Express 16 (15) (2008) 11405.
[7] M. Scalora et al., Phys. Rev. Lett. 73 (10) (1994) 1368.
[8] L. Brzozowski, E. Sargent, IEEE J. Quant. Electron. 36 (5) (2000) 550.
[9] E. Johnson, E.H. Sargent, IEEE J. Lightw. Technol. 20 (8) (2002) 234.
[10] D. Pelinovsky, J. Sears, L. Brzozowski, E.H. Sargent, J. Opt. Soc. Am. B 19 (1) (2002) 43.
[11] L. Brzozowski, E.H. Sargent, IEEE J. Quant. Electron. 36 (11) (2000) 1237.
[12] L. Brzozowski, V. Sukhovatkin, E.H. Sargent, A.J. Spring Thorpe, M. Extavour, IEEE J. Quant. Electron. 39 (7) (2003) 924.
[13] D.E. Pelinovsky, L. Brzozowski, E.H. Sargent, Phys. Rev. E 62 (2000) (R4536–R4539).
[14] L. Brzozowski, E.H. Sargent, J. Opt. Soc. Am. B (2000) 1360.
[15] L. Brzozowski et al., IEEE J. Quant. Electron. 39 (7) (2003) 924.
[16] H. Zoweil, J. Lit, Opt. Commun. 212 (1–3) (2002) 57.
[17] H. Haug (Ed.), Optical Nonlinearities and Instabilities in Semiconductor, Academic Press, Inc., San Diego, 1988.
[18] B.R. Bennett, R.A. Soref, J.A.D. Alamo, IEEE J. Quant. Electron. 26 (1) (1990) 113.
[19] S. Leonard, H. van Driel, J. Schilling, R. Wehrspohn, Phys. Rev. B 66 (161102) (2002) 1.
[20] J. Dow, D. Redfield, Phys. Rev. B 5 (1972) 594.
[21] J.I. Pankove, Phys. Rev. 140 (6a) (1965) A2059.
[22] J. Carrol, J. Whiteaway, D. Plumb, Distributed Feedback Semiconductor Lasers, SPIE Optical Engineering Press, London, 1998.
[23] J.P. Weber, IEEE J. Quant. Electron. 30 (8) (1994) 1801.